


Canadian Field Soils IV: Modeling Thermal Conductivity at Dryness and Saturation

V. R. Tarnawski¹ · M. L. McCombie¹ ·
W. H. Leong² · P. Coppa³ · S. Corasaniti³ ·
G. Bovesecchi³ 

Received: 18 June 2017 / Accepted: 30 December 2017 / Published online: 16 January 2018
© Springer Science+Business Media, LLC, part of Springer Nature 2018

Abstract The thermal conductivity data of 40 Canadian soils at dryness (λ_{dry}) and at full saturation (λ_{sat}) were used to verify 13 predictive models, i.e., four mechanistic, four semi-empirical and five empirical equations. The performance of each model, for λ_{dry} and λ_{sat} , was evaluated using a standard deviation (SD) formula. Among the mechanistic models applied to dry soils, the closest λ_{dry} estimates were obtained by MaxRTCM ($SD = \pm 0.018 \text{ Wm}^{-1} \cdot \text{K}^{-1}$), followed by de Vries and a series-parallel model (S-||). Among the semi-empirical equations (deVries-ave, Advanced Geometric Mean Model (A-GMM), Chaudhary and Bhandari (C-B) and Chen's equation), the closest λ_{dry} estimates were obtained by the C-B model ($\pm 0.022 \text{ Wm}^{-1} \cdot \text{K}^{-1}$). Among the empirical equations, the top λ_{dry} estimates were given by CDry-40 ($\pm 0.021 \text{ Wm}^{-1} \cdot \text{K}^{-1}$ and $\pm 0.018 \text{ Wm}^{-1} \cdot \text{K}^{-1}$ for 18-coarse and 22-fine soils, respectively). In addition, λ_{dry} and λ_{sat} models were applied to the λ_{sat} database of 21 other soils. From all the models tested, only the maxRTCM and the CDry-40 models provided the closest λ_{dry} estimates for the 40 Canadian soils as well as the 21 soils. The best λ_{sat} estimates for the 40-Canadian soils and the 21 soils were given by the A-GMM and the S-|| model.

Keywords Database · Dry soils · Predictive models · Saturated soils · Thermal conductivity · Validation

✉ G. Bovesecchi
gianluigi.bovesecchi@gmail.com

¹ Division of Engineering, Saint Mary's University, Halifax, Canada

² Department of Mechanical and Industrial Engineering, Ryerson University, Toronto, Canada

³ Department of Industrial Engineering, University of Rome "Tor Vergata", 00133 Rome, Italy

List of symbols

Latin

f_{sc}	Inter-particle cementation factor
g	Shape value
i	Soil solid component
j	Total number of soil solid components
k	Shape factor
m_{cl}	Mass fraction of clay particles
m_{sa}	Mass fraction of sand particles
m_{si}	Mass fraction of silt particles
n	Soil porosity
n_a	Minuscule portion of air
n_w	Minuscule portion of water
n_{wm}	Total minuscule fraction of air and water
R_{con}	Radius of an elastic inter-particle contact region (m)
R_s	Mean radius of solid particles (m)
R'	Particle roundness
T	Temperature ($^{\circ}\text{C}$)

Greek

α	Contact resistance factor
β	Cubic cell model coefficient
ε	Inter-particle contact coefficient
ζ	Phase weighting factor
θ	Volumetric fraction
Θ	Volumetric mineral content
λ	Thermal conductivity ($\text{Wm}^{-1} \cdot \text{K}^{-1}$)
ρ	Particle density ($\text{kg} \cdot \text{m}^{-3}$)
Ψ	Particle shape (maxRTCM)

Subscripts

a	Air
ave	Average
b	Bulk
cal	Calculated
cl	Clay
con	Contact
cor	Correlation
dry	Dryness
eff	Effective
exp	Experimental
f	Fluid (air or water)
o-min	Other minerals
qtz	Quartz

r	Radiation
s	Soil solids
sa	Sand
sat	Saturation
sat-coarse	Saturated coarse soils
sat-fine	Saturated fine soils
sb	Solid bridged
si	Silt
u	Fitting parameter in C–B model
w	Water
z	Constant in C–K model

Symbol

	Parallel
⊥	Perpendicular

Abbreviation

A-GMM	Advanced geometric mean model
C–B	Chaudhary and Bhandari model
CDry-40	40-Canadian dry soils
C–K	Côté–Konrad model
CSat-18	18-Canadian saturated coarse soils
CSat-22	22-Canadian saturated fine soils
GMM	Geometric mean model
GSC	Gaylon Sanford Campbell model
Ke	Kersten’s non-dimensional function
LRGH	Lu–Ren–Gong–Horton model
M	number of model fitting parameters
MaxRTCM	Maxwellian Regolith thermal conductivity model
N	number of independent λ records
S-	Series-parallel model
SD	Standard deviation
S_r	Degree of saturation
SSA	Soil specific area

Canadian Provinces—soil codes

AB	Alberta
BC	British Columbia
MN	Manitoba
NB	New Brunswick
ON	Ontario
PE	Prince Edward Island
QC	Québec
NS	Nova Scotia
SK	Saskatchewan

1 Introduction

Thorough knowledge of soil thermal conductivity (λ) is essential in modeling ground temperature (T) regimes in the vicinity of earth-contact facilities dissipating heat, such as buried power cables, ground heat exchangers, pipelines, building foundations, etc. [1]. For example, underground high voltage power cables release a substantial amount of heat that must be dissipated to the surrounding ground in order to avoid overheating and consequent undesirable failure. Therefore, knowledge of the soil ability to conduct heat plays a key role in the design and operation of buried power cables, nuclear waste disposal, underground soil heating, etc. Coarse soils are commonly used as backfill materials around ground-contact devices; this is due to a large content of quartz in these soils and their capability for denser compaction. In general, the flow of heat in soils is influenced by their porosity (n), soil fluid (air and/or water) in soil void space, inter-particle contact resistance and mineral composition of a solid phase. As a result, soil λ is primarily influenced by thermal conductivities of each phase, air (a): $\lambda_a \approx 0.026 \text{ Wm}^{-1} \cdot \text{K}^{-1}$; water (w): $\lambda_w \approx 0.61 \text{ Wm}^{-1} \cdot \text{K}^{-1}$ [1]; solids (s): $\lambda_s \approx 2.2 \text{ Wm}^{-1} \cdot \text{K}^{-1}$ – $7.7 \text{ Wm}^{-1} \cdot \text{K}^{-1}$ [2]; and their volumetric fractions (θ_a , θ_w and θ_s). In general, dry soils ($\theta_w = 0$) have a low thermal conductivity (λ_{dry}) and can consequently act like an insulating medium causing a temperature increase in insulating applications; in addition, λ_{dry} decreases with increasing n . Due to the presence of these important factors, modeling a ground domain, with buried, heat releasing engineering devices, is a complex problem and the obtained results are often unreliable mainly due to a lack of consolidated soil λ data. Measuring λ is time consuming and expensive due to the enormous complexity and variability of soil structure, intricate heat and mass transfer phenomena [3,4], and limitations of measuring techniques and manufactured devices. Consequently, a prevailing majority of research concentrates on λ modeling rather than obtaining this property through measurements. One frequently used approach to λ modeling is a normalized expression, $Ke = (\lambda - \lambda_{\text{dry}})/(\lambda_{\text{sat}} - \lambda_{\text{dry}})$ [2]; where Ke is an empirical, non-dimensional function ($0 \leq Ke \leq 1$) that depends on the degree of saturation (S_r) and soil texture. Subsequently, λ estimates are obtained from a simple relation, $\lambda = \lambda_{\text{dry}} + Ke(\lambda_{\text{sat}} - \lambda_{\text{dry}})$, that requires knowledge of reliable λ data at soil dryness (λ_{dry}) and full saturation (λ_{sat}). In dry soils, heat is mainly transmitted by conduction through the soil minerals, inter-particle contacts, and air. The path of heat transfer through inter-particle contacts is difficult to examine analytically due to unpredictable soil structure and complex particle shapes. However, inter-particle soil contacts have a strong impact on the amount of heat transferred and, therefore, should not be completely disregarded [5,6]. Consequently, modeling λ_{dry} remains a challenging task. As a result, there is a continuous demand for more complete λ_{dry} models that should also include models that exclusively apply to standard pure quartz sands [5,7]. The majority of existing λ_{dry} models are semi-empirical or purely empirical, e.g., Yun and Santamarina [5], Chaudhary and Bhandari [8], Campbell [9], Chen [10], Côté and Konrad [11], and Lu et al. [12]. The application of these models is usually limited to the soils and measuring conditions for which they were fitted to. In addition, these models do not use physical parameters associated with conduction heat flow in dry soils, such as, λ_s , λ_a , shapes of soil particles, inter-particle thermal contact resistance. More versatile λ_{dry} models are those of a mechanistic nature such

as, a weighted average λ model, initially proposed by de Vries [13] and then simplified by Johansen [2]; a series-parallel (S-||) model for two-phase soils, originally proposed by Woodside and Messmer [14] and later modified by Kasubuchi et al. [15]; a new S-|| model applied to three-phase soils in a full S_r range proposed by Tarnawski and Leong [16]; a model that uses an array of cubic cells representing three-phase granular materials developed by Gori and Corasaniti [17, 18]; and a framework λ model (MaxRTCM) for porous planetary regolith by Wood [19] that includes an inter-particle contact factor in unconsolidated planetary dust, soil and mineral fragments covering bedrock.

Assessments of λ_{sat} are usually obtained by a geometric mean model (GMM), $\lambda_{\text{sat}} = \lambda_s^{1-n} \lambda_w^n$, that usually produces acceptable λ estimates of experimental data. Other models, also valid to saturated soils, are: Chaudhary and Bhandari [8], Campbell [9], de Vries [13], Gori and Corasaniti [17, 18], and Tarnawski et al. [16, 20].

In summary, a large majority of λ_{dry} and λ_{sat} models are of empirical or semi-empirical nature. These models rarely produce satisfactory estimates on soil data other than that they were fitted to. In addition, a majority of these models lack the inclusion of conduction heat transfer through inter-particle contacts [21, 22]. In turn, the mechanistic models appear to be, at first glance, more versatile as they include a simplified soil structure combined with some elements of heat flow. On the other hand, they are rather intricate to use and often lack accurate and unbiased predictions. For that reason, an independent validation of the published models, with respect to a complete soil λ database, still remains an unachieved goal. Therefore, the objective of this paper is to review modeling approaches to λ_{dry} and λ_{sat} followed by a critical analysis of their estimates with respect to the published database of 40 Canadian soils [23].

2 Thermal Conductivity Database of Canadian Dry and Saturated Soils

Forty Canadian soil samples, ranging from coarse sands to fine clays, were tested in laboratory conditions for their ability to conduct heat using a non-stationary probe technique [23]. The measurements were taken on compacted soil samples, at room T of about 25 °C, and at a full range of S_r from dryness ($S_r = 0$) to full saturation ($S_r = 1$). Due to a wide diversity in soil texture, the entire database was split into two soil textural groups, namely: coarse soils, with a mass fraction of sand ($m_{\text{sa}} \geq 0.40$), and fine soils ($m_{\text{sa}} < 0.40$). Physical characteristics of both soil textures are shown in Table 1 (Coarse Soils) and Table 2 (Fine Soils). Each record of λ_{dry} and λ_{sat} represents an average value of nine λ measurements taken from three separate soil samples of approximately the same n and T . More details about Canadian field soils, measurements and λ database were given by Tarnawski et al. [23]. A graphical display of λ_{dry} and λ_{sat} versus n is shown in Figs. 1 and 2, respectively.

From Fig. 1, a declining trend of λ_{dry} with increasing n was noted and it was approximately linear; λ_{dry} varied approximately from $0.13 \text{ Wm}^{-1} \cdot \text{K}^{-1}$ to $0.30 \text{ Wm}^{-1} \cdot \text{K}^{-1}$. Also, for a large majority of saturated soils, a roughly linearly declining trend of λ_{sat} versus n is also observed (Fig. 2); however, λ_{sat} varies roughly from $1.0 \text{ Wm}^{-1} \cdot \text{K}^{-1}$ to $3.2 \text{ Wm}^{-1} \cdot \text{K}^{-1}$.

Table 1 18 Canadian coarse soils—physical characteristics

Coarse soils ($m_{sa} \geq 0.40$)						
Soil code	m_{sa}	ρ_b (kg · m ⁻³)	n	λ_{dry} (Wm ⁻¹ · K ⁻¹)	λ_{sat} (Wm ⁻¹ · K ⁻¹)	
NS-04	1.00	1728	0.36	0.30		3.17
QC-01	0.93	1539	0.43	0.21		1.59
ON-04	0.89	1647	0.39	0.26		1.67
NS-05	0.85	1620	0.4	0.27		2.39
ON-06	0.84	1512	0.44	0.24		1.60
PE-03	0.83	1593	0.41	0.30		1.98
SK-04	0.83	1566	0.42	0.22		1.82
MN-04	0.81	1431	0.47	0.22		1.93
QC-02	0.79	1404	0.48	0.21		1.57
ON-03	0.71	1458	0.46	0.21		1.52
SK-05	0.68	1485	0.45	0.23		1.84
SK-02	0.67	1485	0.45	0.23		1.73
NS-02	0.61	1485	0.45	0.25		1.93
NS-03	0.57	1620	0.4	0.29		2.17
NS-06	0.56	1323	0.51	0.21		1.76
ON-05	0.56	1674	0.38	0.25		1.74
PE-02	0.51	1566	0.42	0.29		1.94
PE-01	0.50	1512	0.44	0.26		1.92

3 Specifics of Published Modeling Approaches

Several λ models for soils were developed in the past with detailed reviews given by Farouki [1], Côté and Konrad [24], and Tarnawski et al. [25]. Mechanistic models are usually complex in form, but for dry ($\theta_w = 0$) and saturated ($\theta_w = n$) conditions, their forms are greatly simplified. Moreover, if the soil mineral composition is not available, the thermal conductivity of solids (λ_s) is a fitting parameter in all the mechanistic and semi-empirical models.

3.1 Assessment of the Mechanistic Models

Mechanistic models are based on the basic principles of conduction heat transfer in porous media comprised of solids, air and water. In theory, mechanistic models should not require any fitting parameters. However, in reality, some mechanistic models use several theoretical coefficients that are often cumbersome to determine. As a result, these coefficients are usually obtained by fitting the models to experimental data [13]. Therefore, these models are prone to a subjective validation, particularly if the λ database used is incomplete. Furthermore, these models use a simplified soil structure; often, they do not consider heat transfer through inter-particle contacts [14–18].

Table 2 22 Canadian fine soils—physical characteristics

Fine soils ($m_{sa} < 0.40$)					
Soil code	m_{sa}	$\rho_b(\text{kg} \cdot \text{m}^{-3})$	n	$\lambda_{dry} (\text{Wm}^{-1} \cdot \text{K}^{-1})$	$\lambda_{sat} (\text{Wm}^{-1} \cdot \text{K}^{-1})$
AB-01	0.38	1215	0.55	0.18	1.39
ON-01	0.37	1539	0.43	0.31	1.60
NS-01	0.32	1215	0.55	0.18	1.46
BC-06	0.32	1296	0.52	0.19	1.43
ON-07	0.32	1485	0.45	0.25	1.46
NB-04	0.26	1242	0.54	0.15	1.31
NB-03	0.24	1026	0.62	0.13	1.14
MN-02	0.22	1593	0.41	0.27	2.19
NS-07	0.22	1161	0.57	0.18	1.40
MN-01	0.17	1215	0.55	0.19	1.43
ON-02	0.07	1323	0.51	0.20	1.16
NB-01	0.03	1242	0.54	0.18	1.46
MN-03	0.03	999	0.63	0.15	1.05
SK-03	0.02	1269	0.53	0.19	1.27
NB-02	0.00	1188	0.56	0.16	1.35
BC-05	0.00	1269	0.53	0.19	1.14
NB-05	0.00	1242	0.54	0.20	1.46
SK-01	0.00	1593	0.41	0.28	1.97
BC-01	0.00	1323	0.51	0.21	1.20
BC-02	0.00	1350	0.5	0.20	1.21
BC-03	0.00	1323	0.51	0.20	1.30
BC-04	0.00	1296	0.52	0.19	1.12

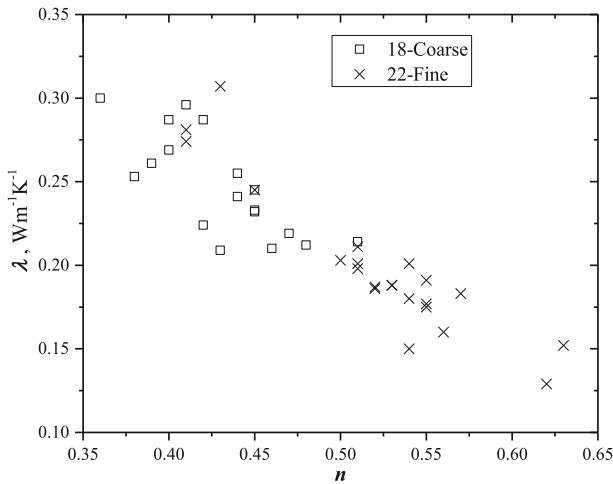


Fig. 1 40 Canadian dry soils: variation of λ_{dry} versus n

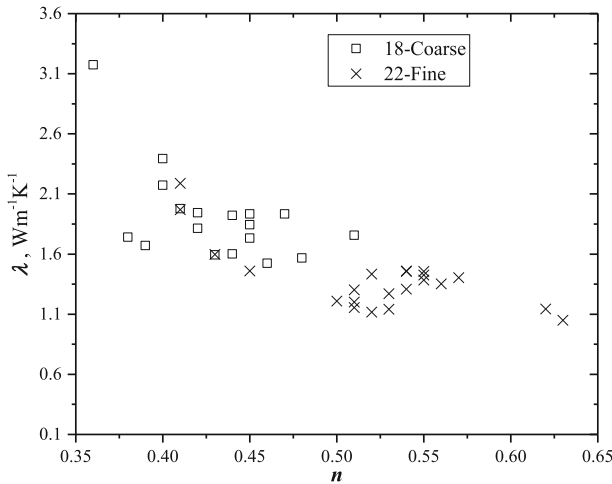


Fig. 2 40 Canadian saturated soils: variation of λ_{sat} versus n

3.1.1 deVries Model [13]

Soil λ is modeled as the weighted average of soil components with their shape factors (k), λ and corresponding volume fractions (θ).

$$\lambda = \frac{k_w \cdot \lambda_w \cdot \theta_w + \sum_1^j k_i \cdot \lambda_i \cdot \theta_i + k_a \cdot \lambda_a \cdot \theta_a}{k_w \cdot \theta_w + \sum_1^j k_i \cdot \theta_i + k_a \cdot \theta_a} \tag{1}$$

The soil structure is assumed to be composed of ellipsoidal grains freely floating in a continuous medium of air and/or water, i.e., the soil grains do not touch each other. If all soil grains are lumped into one solid phase (s), then Eq. 1 converts to the following form:

$$\lambda = \frac{k_w \lambda_w \theta_w + k_s \lambda_s \theta_s + k_a \lambda_a \theta_a}{k_w \theta_w + k_s \theta_s + k_a \theta_a} \tag{2}$$

where $\theta_s = \rho_b / \rho_s$; $\theta_s + \theta_a + \theta_w = 1$; ρ_s is the solid (mineral) density; and k_s, k_a, k_w are the shape factors of solids, air and water.

For dry conditions ($\theta_w = 0, k_w = 0, \theta_a = n, k_a = 1$), Eq. 2 converts to the following form:

$$\lambda_{dry} = \lambda_a \frac{\rho_s + \rho_b \left(k_s \frac{\lambda_s}{\lambda_a} - 1 \right)}{\rho_s + \rho_b (k_s - 1)} = \lambda_a \frac{n + (1 - n) k_s \frac{\lambda_s}{\lambda_a}}{n + (1 - n) k_s} \tag{3}$$

where k_s is given by:

$$k_s = \frac{1}{3} \left[\frac{2}{1 + (\lambda_s / \lambda_a - 1) g_s} + \frac{1}{1 + (\lambda_s / \lambda_a - 1) (1 - 2g_s)} \right] \tag{4}$$

where g_s is a soil particle shape value (a fitting parameter of 0.125 [13]) and λ_s is the thermal conductivity of solids.

According to de Vries [13], the use of Eq. 4 is restricted by the following conditions:

1. Soil grains are treated as rotated ellipsoids.
2. The ellipsoids are far apart, so that they do not impact each other.

The first condition is roughly acceptable for coarse soils, while it is objectionable for fine soils composed mainly of flat, tiny particles (i.e., lamellae). This could be a major reason of generally reduced the model performance when it is applied to fine soils. The second condition is also not fulfilled in soils and it is a major reason behind a correction factor introduced by de Vries [13]. The λ_s was estimated by the geometric mean of λ of quartz (λ_{qtz}) and other minerals (λ_{o-min}) [2]: $\lambda_s = \lambda_{qtz}^{\theta_{qtz}} \lambda_{o-min}^{1-\theta_{qtz}} = \lambda_{qtz}^{\theta_{qtz}} \lambda_{o-min}^{1-\theta_{qtz}}$. Where, $\lambda_{o-min} \approx 2 - 2.2 \text{ Wm}^{-1} \cdot \text{K}^{-1}$ and $\lambda_{qtz} \approx 7.7 \text{ Wm}^{-1} \cdot \text{K}^{-1}$.

Equation 3 produces a nearly linear increase of λ_{dry} with increasing ρ_b at large soil n ; while at small n , a noticeable increase of λ_{dry} was noted [1]. The deVries Model, in its original version (Eqs. 2 and 3), uses $\lambda_{qtz} = 8.8 \text{ Wm}^{-1} \cdot \text{K}^{-1}$ and in spite of that it underestimates λ ; consequently, a multiplication factor of 1.25 was recommended [13].

For saturated soil conditions ($\theta_w = n, \theta_a = 0, k_a = 0, k_w = 1$), Eq. 2 converts to the following form:

$$\lambda_{sat} = \lambda_w \frac{1 + (1 - n)(k_s \lambda_s / \lambda_w - 1)}{1 + (1 - n)(k_s - 1)} \tag{5}$$

where k_s is given by:

$$k_s = \frac{1}{3} \left[\frac{2}{1 + (\lambda_s / \lambda_w - 1) g_s} + \frac{1}{1 + (\lambda_s / \lambda_w - 1) (1 - 2g_s)} \right] \tag{6}$$

Further discussion regarding adaptation of this model to soil environment is given in Sect. 5.

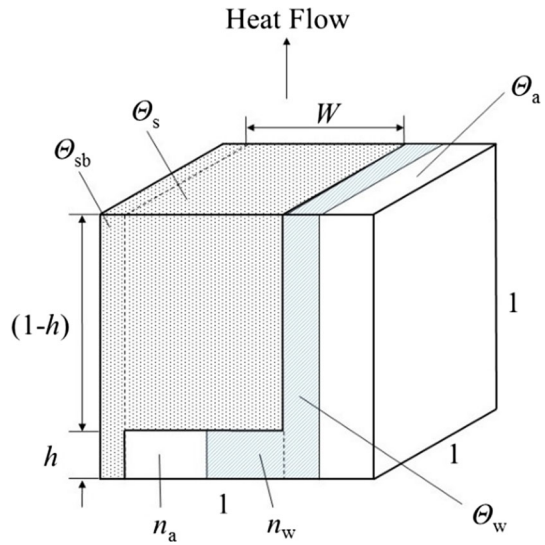
3.1.2 Series-Parallel Models (S-||) Models [14–16]

The basic soil constituents (solids, air and water) are arranged in either series or parallel with respect to heat flow. In fact, these arrangements establish the upper or lower bounds of effective thermal conductivity (λ_{eff}), respectively. Woodside published the first S-|| model for two-phase granular systems, and Messmer [14] assumed two parallel paths of heat flow. The first path, through soil air as a continuous medium, and the second path, along solid grains bridged with tiny volumes of soil air in series. However, the second path disregards heat flow through inter-particle contacts. Later, Kasubuchi et al. [15] applied this model (Eq. 7) to three dry Japanese soils.

$$\lambda_{dry} = \lambda_a (n - n_{wm}) + \frac{(1 - n + n_{wm})^2}{(1 - n) / \lambda_s + n_{wm} / \lambda_a} \tag{7}$$

where n_a is the air fraction in a series path of heat flow. See above equation.

Fig. 3 Schematic representation of three paths of heat flow in a partitioned soil cubic cell



Then, Tarnawski and Leong [16] developed an S-|| model applied to a full range of S_r (three-phase granular materials). In a partitioned cubic cell (Fig. 3), representing a piece of soil, heat is conducted through three pathways, namely a solid uniform passage (Θ_{sb}), a series-parallel passage composed of solids bridged with a parallel path of minuscule portion of soil water (n_w) and a minuscule portion of soil air (n_a) and, finally, a path of water (Θ_w) and air (Θ_a) in a parallel arrangement. In fact, Θ_{sb} and $n_{wm} = n_a + n_w$ are fitting parameters.

By applying a classical resistor model to each heat pathway, the following expression was obtained:

$$\lambda_{S-||-||} = \lambda_s \Theta_{sb} + \frac{(1 - n - \Theta_{sb} + n_{wm})^2}{\frac{1-n-\Theta_{sb}}{\lambda_s} + \frac{n_{wm}}{\lambda_w \frac{n_w}{n_{wm}} + \lambda_a (1 - \frac{n_w}{n_{wm}})}} + \lambda_w \left(n S_r - n_{wm} \frac{n_w}{n_{wm}} \right) + \lambda_a \left[n - n_{wm} - \left(n S_r - n_{wm} \frac{n_w}{n_{wm}} \right) \right] \tag{8}$$

where $n_{wm} = n_a + n_w$ is the total fraction of minuscule soil pore space.

For dry conditions ($S_r = 0$):

$$\lambda_{dry} = \lambda_s \Theta_{sb} + \frac{(1 - n - \Theta_{sb} + n_{wm})^2}{\frac{1-n-\Theta_{sb}}{\lambda_s} + \frac{n_{wm}}{\lambda_a}} + \lambda_a (n - n_{wm}) \tag{9}$$

For saturated conditions ($S_r = 1$):

$$\lambda_{sat} = \lambda_s \Theta_{sb} + \frac{(1 - n - \Theta_{sb} + n_{wm})^2}{\frac{1-n-\Theta_{sb}}{\lambda_s} + \frac{n_{wm}}{\lambda_w}} + \lambda_w (n - n_{wm}) \tag{10}$$

The model was calibrated using λ data of five soils representing coarse, medium, and fine textures. Two structural characteristics of the elemental soil cell, n_{wm} and Θ_{sb} , can be obtained from the following relations:

$$n_{wm} = 0.088 - 0.037m_{sa}^3 \quad (11)$$

$$\Theta_{sb} = 0.0237 - 0.0175m_{sa}^3 \quad (12)$$

Further details regarding adaptation of this model to soil environment is given in Sect. 5.

3.1.3 Cubic Cell [17]

A structure of dry/saturated soils was assumed as an array of infinitesimal cubical cells; each containing a centrally positioned dice representing lumped soil solids, while the space surrounding the solid core was filled with air or water. The effective λ_{eff} was estimated from the following relation:

$$\frac{1}{\lambda_{eff}} = \frac{\beta - 1}{\lambda_f \cdot \beta} + \frac{\beta}{\lambda_s + \lambda_f \cdot [\beta^2 - 1]} \quad (13)$$

where $\beta = \sqrt[3]{1/(1-n)}$; at $S_r = 0$: $\lambda_f = \lambda_a$ and $\lambda_{eff} = \lambda_{dry}$; and at $S_r = 1$: $\lambda_f = \lambda_w$ and $\lambda_{eff} = \lambda_{sat}$.

Recently, this model was revised [18] and a spherical shape of soil grains was introduced.

3.1.4 MaxRTCM [19]

It is an analytical model that estimates λ_{eff} of dry planetary regolith (fine-grained soil covering a solid bedrock). The model consisted of the thermal conductivity of solid material (λ_s), system porosity (n), non-spherical particle size and shape (Ψ), a factor representing an inter-particle cementation (f_{sc}) and radiation heat transfer between particles surrounded by a vacuum (λ_r). Particle shape was described by its spherical nature and roundness.

$$\lambda_{\text{eff}} = \lambda_s f_{\text{sc}} \frac{\left(\frac{3}{\Psi} - 1\right) (1 - n)}{\frac{3}{\Psi} - (1 - n)} + \lambda_r (1 - f_{\text{sc}}) \frac{\frac{3}{\Psi} (1 - n) + n}{n} \quad (14)$$

The inter-particle cementation, f_{sc} , is an empirical factor that represents a fractional continuity of the high conductivity phase, ranging from 0 to 1 : $f_{\text{sc}} = 0.6 (R_{\text{con}}/R_s)$, where R_{con} is the radius of an elastic contact region between particles and R_s is the mean radius of solid particles. In general, λ_s , Ψ and f_{sc} are difficult to determine analytically; therefore, they are usually treated as fitting parameters. Further discussion regarding adaptation of this model to soil environment is given in Sect. 5.

3.2 Review of the Semi-empirical Models

Semi-empirical models are a transitional class of models between the mechanistic and empirical types. These models use some implicit principles of heat transfer combined with experimental data; no soil structure is considered in their function; usually, they contain at least one fitted parameter.

3.2.1 deVries-ave [13]

Johansen [2] simplified Eq. (3) to a more practical form for handling data of field soils. The unknown coefficients of the model by de Vries (Eq. 3) were obtained by fitting to λ data of soils studied by Kersten [26], namely, soil particle shape values $g_1 = g_2 = 0.1$ and $g_3 = 0.8$; thermal conductivity of solids $\lambda_s = 3 \text{ Wm}^{-1} \cdot \text{K}^{-1}$ and the shape factor of solids $k_s = 0.053$. Other fixed coefficients were also introduced, such as, $\rho_s = 2700 \text{ kg} \cdot \text{m}^{-3}$, $\lambda_{\text{qtz}} = 7.69 \text{ Wm}^{-1} \cdot \text{K}^{-1}$ and $\lambda_a = 0.024 \text{ Wm}^{-1} \cdot \text{K}^{-1}$. After substituting the above coefficients into Eq.(3), the following simplified expression was obtained:

$$\lambda_{\text{dry}} = \frac{A\rho_b + B}{\rho_s - C\rho_b} = \frac{A(1 - n)\rho_s + B}{\rho_s - C(1 - n)\rho_s} \quad (15)$$

where $A = \lambda_a \cdot (k_s \cdot \frac{\lambda_s}{\lambda_a} - 1) = 0.135$; $B = \lambda_a \cdot \rho_s = 64.8$; and $C = (1 - k_s) = 0.947$.

The additional fitting parameter was a soil particle shape value g_s upon which k_s is calculated (Eq. (6)). In spite of a fixed λ_s of $3 \text{ Wm}^{-1} \cdot \text{K}^{-1}$, Eq. (15) has been commonly applied to field soils regardless of their texture and mineral composition [1]. It is also worth noting that some of Kersten's soils were of volcanic origin (Alaska) and hence, their physical properties were usually different from those of mineral soils. Further discussion regarding adaptation of this model to Canadian Soils is provided in Sect 5.

3.2.2 Advanced Geometric Mean Model (A-GMM) [20]

When the classical geometric mean model (Eq. 16) is applied to dry soils, it largely over-predicts experimental data.

$$\lambda_{\text{dry}} = \lambda_s^{1-n} \cdot \lambda_a^n \quad (16)$$

Therefore, in spite of its simplicity, this model is not used for dry soils due to a large ratio of $\lambda_s/\lambda_a \approx 100 - 300$ and also due to the fact that the thermal contact resistance at the inter-particle level is missing. Recently, Tarnawski and Leong [20] successfully introduced inter-particle contact resistance factors (α_{dry} and α_{sat}) in the classical geometric mean model.

$$\lambda_{dry} = [\alpha_{dry} \cdot \lambda_s]^{1-n} \cdot [\lambda_a]^n \tag{17}$$

For saturated conditions:

$$\lambda_{sat} = [\alpha_{sat} \lambda_s]^{1-n} \cdot [\lambda_w]^n \tag{18}$$

where $\alpha = \left[\varepsilon + (1 - \varepsilon) \frac{\lambda_s}{\lambda_f} \right]^{-1}$; at $S_r = 0$: $\alpha = \alpha_{dry}$ and $\lambda_f = \lambda_a$; and at $S_r = 1$: $\alpha = \alpha_{sat} = 1$ and $\lambda_f = \lambda_w$.

The advanced geometric mean model (A-GMM) also introduces a dimensionless inter-particle contact coefficient (ε). According to Tarnawski et al. [20], ε mainly depends on soil texture. The soil specific area (SSA) is inversely proportional to the soil grain size, i.e., on average, small soil particles have a larger SSA than for the same mass made up of large particles. Also, the particle shape appears to be interrelated with SSA; flattened or elongated particles (fine soils) have a greater SSA than spherical or cubical particles (coarse soils). Therefore, fine soils have a larger ε than coarse soils. However, due to irregular soil inter-particle structure, there is no analytical relation for ε . Therefore, ε is a fitting parameter. Further details, regarding adaptation of this model to Canadian Soils is provided in Sect. 5.

3.2.3 Chaudhary–Bhandari (C–B) [8]

This model is another adaptation of the weighted geometric mean model to three-phase porous media. It combines $\lambda_{||}$ (in the parallel direction to heat flow), λ_{\perp} (in the perpendicular direction to heat flow) and a phase weighting factor ζ [8].

$$\lambda_{eff} = \lambda_{||}^{\zeta} \lambda_{\perp}^{1-\zeta} \tag{19}$$

where $\lambda_{||} = n\lambda_f + (1 - n)\lambda_s$ and $\lambda_{\perp} = [n\lambda_f + (1 - n)\lambda_s]^{-1}$

The model assumes that the ζ fraction of the porous media is oriented in parallel to the direction of heat flow, while the $1 - \zeta$ fraction is oriented in perpendicular to the heat flow.

For two-phase unconsolidated soils (i.e., at dry and/or saturated state), the above relation can be written as follows:

$$\lambda_{eff} = \lambda_s^{1+\zeta} \lambda_f^{1-\zeta} \frac{[n(1 - n)]^{\zeta}}{n\lambda_s + (1 - n)\lambda_f} \tag{20}$$

where ζ is assessed from $\zeta = u(1 - \log n)/\log [n(1 - n)\lambda_s/\lambda_a]$ with $u = 0.5$ as a fitting parameter.

Further details regarding adaptation of this model to Canadian Soils is given in Sect. 5.

3.2.4 Chen's Equations [10]

The λ data of four unsaturated sands (pure quartz) showed an exponential λ dependence on n and the following equation was given:

$$\lambda = \lambda_s^{1-n} \lambda_w^n [(1 - 0.0022) S_r + 0.0022]^{0.78n} \tag{21}$$

However, at $S_r = 0$, the air component (λ_a) is missing, while λ_w is present. It is likely that λ_a is hidden in the constant of 0.0022 ($\approx 0.0846 \cdot \lambda_a$). The following equation was obtained by substituting $0.0846 \cdot \lambda_a$ and $\lambda_w = 0.61 \text{ Wm}^{-1} \cdot \text{K}^{-1}$.

$$\lambda_{\text{dry}} = \lambda_s^{1-n} [0.61 (0.0846\lambda_a)^{0.78}]^n = \lambda_s^{1-n} [0.089\lambda_a^{0.78}]^n \tag{22}$$

At $S_r = 1$, Eq. (21) can be simplified to the geometric mean form:

$$\lambda_{\text{sat}} = \lambda_{\text{qtz}}^{1-n} \lambda_w^n \tag{23}$$

3.3 Review of the Empirical Equations

These models are obtained directly by fitting experimental data of λ versus n . The obtained equations are relatively simple, e.g., 1st and 2nd order polynomials with n as the input parameter.

3.3.1 GSC [9]

The following empirical equation was fitted to λ data of five soils from Eastern Washington (USA).

$$\lambda = A + B\theta_w - (A - D) \exp[-(C\theta_w)^E] \tag{24}$$

where A, B, C, D and E are fitting coefficients and θ_w is volumetric water content.

For dry soils, $\theta_w = 0$, the following expression is applied:

$$\lambda_{\text{dry}} = 0.03 + 0.7(1 - n)^2 \tag{25}$$

For saturated soils, $\theta_w = n$, the last term in Eq. (24) is zero, so that

$$\lambda_{\text{sat}} = A + Bn \tag{26}$$

where $A = \frac{0.57/(1-n)+1.73\theta_{\text{qtz}}+0.93(1-\theta_{\text{qtz}})}{1/(1-n)-0.74\theta_{\text{qtz}}-0.49(1-\theta_{\text{qtz}})} - 2.8n(1 - n)$ and $B = 2.8(1 - n)$

3.3.2 Côté–Konrad (C–K) [11]

The thermal conductivity at dryness, λ_{dry} , is estimated from a fitted relation dependent on n and two other parameters (λ_x and b) accounting for λ_s and soil grain shape.

$$\lambda_{\text{dry}} = \lambda_x 10^{-z \cdot n} \quad (27)$$

where $\lambda_x = 0.75 \text{ Wm}^{-1} \cdot \text{K}^{-1}$ and $z = 1.2$

3.3.3 LRGH [12]

The following n dependent empirical relation for λ_{dry} was proposed for 10 Chinese soils.

$$\lambda_{\text{dry}} = -0.56n + 0.51 \quad (28)$$

3.3.4 Yun–San [5]

For pure quartz sands, the following equation was proposed.

$$\lambda_{\text{dry}} = -0.291 \ln(n) + 0.026 \quad (29)$$

A quick reference summary for all the models is given in “Appendix A”.

4 Modeling λ_{dry} and λ_{sat} for 40 Canadian Soils

Using the Database of Canadian 40 Soils, the following empirical equations for λ_{dry} and λ_{sat} were obtained.

4.1 Canadian Soils at Dryness (CDry-40)

A simple λ_{dry} dependence on n was obtained, regardless of soil texture.

$$\lambda_{\text{dry}} = 0.55(1 - n)^{1.4} \quad (30)$$

However, this correlation required two fitting parameters (0.55 and 1.4), i.e., $M = 2$.

4.2 Canadian Coarse Soils at Saturation (CSat-18)

For λ_{sat} data of 18 coarse texture soils, the following correlation was obtained:

$$\lambda_{\text{sat}} = 1.147 + 0.007n^{-5.31} \quad (31)$$

This model required three fitting parameters (1.147, 0.007, and -5.31), i.e., $M = 3$.

4.3 Canadian Fine Soils at Saturation (CSat-22)

For λ_{sat} data of 22 fine texture soils, the following correlation was obtained:

$$\lambda_{\text{sat}} = 1.284 + 13.36 \cdot 10^{-6} n^{-17.484} \quad (32)$$

This model required three fitting parameters (1.284 , $13.36 \cdot 10^{-6}$, and -17.484), i.e., $M = 3$.

5 Adaptation of Published Models to 40 Canadian Soils

5.1 deVries-ave

Direct application of Eq. 15, originally developed for soils by Kersten [26], to λ data of 40 Canadian soils [23] appeared to be uncertain due to noticeably different mineral compositions. Thermal conductivity of solids (λ_s) was a key parameter as it is a lumped value of all minerals in a particular soil. Its numerical value is usually estimated by the geometric mean model [1] applied to all mineral soil components.

$$\lambda_s = \prod_{i=1}^m \lambda_i^{\Theta_i} \quad (33)$$

where Θ_i is the volumetric fraction of the i th soil mineral in soil solids, m is the total number of solid soil minerals and λ_i is the thermal conductivity of the i th soil mineral (for more details, see Appendix).

Application of the above equation to the 40 Canadian soils revealed that λ_s varied from $3.3 \text{ Wm}^{-1} \cdot \text{K}^{-1}$ to $7.7 \text{ Wm}^{-1} \cdot \text{K}^{-1}$ for coarse soils and from $2.5 \text{ Wm}^{-1} \cdot \text{K}^{-1}$ to $4.5 \text{ Wm}^{-1} \cdot \text{K}^{-1}$ for fine soils. Consequently, most λ_s values are higher than $3 \text{ Wm}^{-1} \cdot \text{K}^{-1}$ [2]. Also, the values of soil particle shapes (g_1 , g_2 and g_3) are obtained by fitting calculated λ_{dry} and λ_{sat} to experimental λ data of the 40 Canadian soils. For 18 coarse soils, the following average coefficients were obtained: $\rho_s = 2700 \text{ kg} \cdot \text{m}^{-3}$, $g_1 = g_2 = 0.1$, $g_3 = 0.8$, $\lambda_s = 4.46 \text{ Wm}^{-1} \cdot \text{K}^{-1}$, $\lambda_a = 0.026 \text{ Wm}^{-1} \cdot \text{K}^{-1}$ and $k_s = 0.04$. Substituting these coefficients into Eqs. 3 and 4, the following relation for 18 coarse soils was obtained:

$$\lambda_{\text{dry}} = \frac{A\rho_s \cdot (1 - n) + B}{\rho_s - C\rho_s \cdot (1 - n)} \quad (34)$$

where $\rho_s = 2700 \text{ kg} \cdot \text{m}^{-3}$; $A = \lambda_a \cdot (k_s \cdot \frac{\lambda_s}{\lambda_a} - 1) = 0.145$; $B = \lambda_a \cdot \rho_s = 70.2$ and $C = (1 - k_s) = 0.96$.

For 22 fine soils, the following average coefficients were obtained: $\rho_s = 2700 \text{ kg} \cdot \text{m}^{-3}$, $g_1 = g_2 = 0.053$, $g_3 = 0.894$, $\lambda_s = 3.454 \text{ Wm}^{-1} \cdot \text{K}^{-1}$, $\lambda_{\text{air}} = 0.026 \text{ Wm}^{-1} \cdot \text{K}^{-1}$ and $k_s = 0.088$.

$$\lambda_{\text{dry}} = \frac{A\rho_s \cdot (1 - n) + B}{\rho_s - C\rho_s \cdot (1 - n)} \quad (35)$$

where $\rho_s = 2700 \text{ kg} \cdot \text{m}^{-3}$, $A = \lambda_a \cdot (k_s \cdot \frac{\lambda_s}{\lambda_a} - 1) = 0.157$; $B = \lambda_a \cdot \rho_s = 70.2$; and $C = (1 - k_s) = 0.912$.

For saturated conditions and 18 coarse soils:

$$\lambda_{sat-coarse} = \frac{A\rho_s \cdot (1 - n) + B}{\rho_s - C \cdot \rho_s \cdot (1 - n)} \tag{36}$$

where: $\rho_s = 2700 \text{ kg} \cdot \text{m}^{-3}$; $\lambda_s = 4.46 \text{ Wm}^{-1} \cdot \text{K}^{-1}$; $A = \lambda_w \cdot (k_s \cdot \frac{\lambda_s}{\lambda_w} - 1) = 1.248$; $B = \lambda_w \cdot \rho_s = 1643$; $C = (1 - k_s) = 0.575$.

For saturated conditions and 22 fine soils:

$$\lambda_{sat-fine} = \frac{A\rho_s \cdot (1 - n) + B}{\rho_s - C \cdot \rho_s \cdot (1 - n)} \tag{37}$$

where: $\rho_s = 2700 \text{ kg} \cdot \text{m}^{-3}$; $\lambda_s = 3.454 \text{ Wm}^{-1} \cdot \text{K}^{-1}$; $A = \lambda_w \cdot (k_s \cdot \frac{\lambda_s}{\lambda_w} - 1) = 1.273$; $B = \lambda_w \cdot \rho_s = 1646$; $C = (1 - k_s) = 0.438$.

In general, the predictive performance of the model depends on the number of fitting parameters (M). This model requires one fitting parameter, g_1 (Eq. 6); i.e., $M = 1$.

5.2 C–B

Improved λ_{dry} and λ_{sat} estimates were obtained when u values, applied to the phase weighting factor ζ , were fitted to the 40 Canadian soil data. For dry soils, $u = 0.445$, while for saturated soils, $u = 0.925$. This model requires one fitting parameter, u ; i.e., $M = 1$.

5.3 maxRTCM

Originally, this model was developed for dry, porous and airless planetary regolith, where the presence of radiation heat transfer (λ_r) is dominant. Therefore, for field soils, the model was modified and the following assumptions were made:

(a) For dry field soils $\lambda_a \gg \lambda_r$, was replaced with λ_a :

$$\lambda_{dry} = f_{sc} \frac{(\frac{3}{\Psi} - 1)(1 - n)}{\frac{3}{\Psi} - (1 - n)} \lambda_s + (1 - f_{sc}) \frac{\frac{3}{\Psi}(1 - n) + n}{n} \lambda_a \tag{38}$$

(b) The sphericity of soil particles (Ψ) depends on their roundness (R'). According to Krumbein and Sloss [27]: $0.3 < \Psi < 0.9$, while $0.1 < R' < 0.9$. Due to an endless diversity of soil grain shapes, there is no analytic equation for Ψ . Therefore, it has been defined as a weighted average based on volumetric fractions of sand (θ_{sa}), silt (θ_{si}) and clay (θ_{cl}) and an assumed constant, Ψ , for each major soil fractions, namely, sand ($\Psi_{sa} = 0.865$), silt ($\Psi_{si} = 0.645$) and clay ($\Psi_{cl} = 0.085$).

$$\Psi = \Psi_{sa}\theta_{sa} + \Psi_{si}\theta_{si} + \Psi_{cl}\theta_{cl} \approx 0.865m_{sa} + 0.645m_{si} + 0.085m_{cl} \tag{39}$$

- (c) The solid/cement continuity factor (f_{sc}) depends on the ratio of soil particle contact radius and mean radius of soil particles [19]. However, due to the complexity of soil structure, this specific data are generally not available; consequently, there is no analytical relation for f_{sc} . The missing f_{sc} data were obtained by minimizing the RMSE between experimental λ_{dry} and Eqs. 38 with 39. Then, the obtained f_{sc} values were used to fit a correlation f_{sc-cor} as a function of Ψ and $\ln(\lambda_s/\lambda_a)/(\lambda_s/\lambda_a)$.

$$f_{sc-cor} = \max \left(0, -0.02220 + \frac{0.05520}{\Psi} - \frac{0.03024}{\Psi^2} + 1.4784 \frac{\ln\left(\frac{\lambda_s}{\lambda_a}\right)}{\frac{\lambda_s}{\lambda_a}} \right) \quad (40)$$

It appears that introduction of correlated f_{sc-cor} might be very beneficial to the model performance when applied to dry soils. This model required one fitting parameter (f_{sc-cor}), i.e., $M = 1$.

5.4 A-GMM

A dimensionless inter-particle contact coefficient ε was obtained by fitting Eqs. 17 and 18 to λ data of 18 coarse and 22 fine unsaturated soils [20] and values of 0.988 and 0.996 were obtained, respectively. For λ_{dry} , the model requires one fitting parameter ε , i.e., $M = 1$; while for λ_{sat} the model does not require any fitting as $\alpha_{sat} = 1$.

6 Assessment of Predictive Models

The predictive performance of each λ_{dry} and λ_{sat} model was evaluated with respect to experimental data (λ_{exp}) using the standard deviation value (SD):

$$SD = \sqrt{\frac{1}{N - M} \sum_1^N (\lambda_{exp} - \lambda_{cal})^2} \quad (41)$$

where N is the number of independent λ_{dry} or λ_{sat} records; M is the number of parameters in the model used for fitting to experimental λ data.

A smaller SD means a better performance of the predictive model. Basically, the model predictive performance (i.e., SD) decreases with increasing M .

6.1 Dry Soils

Tables 3 and 4 summarize each model performance for 18 coarse and 22 fine soils, respectively, with both listed according to their performance (SD values).

Table 3 18 dry Canadian soils (coarse)

#	Model name	Model type	Equations	M	SD ($Wm^{-1} \cdot K^{-1}$)
1	MaxRTCM	Mechanistic	38–40	1	± 0.018
2	CDry-40	Empirical	30	2	± 0.021
3	deVries Model	Mechanistic	3, 4	1	± 0.022
4	C–B ($u = 0.445$)	Semi-empirical	20	1	± 0.022
5	deVries-ave	Semi-empirical	34	1	± 0.023
6	GSC	Empirical	25	0	± 0.023
7	C–K	Empirical	27	0	± 0.027
8	A-GMM	Semi-empirical	17	1	± 0.029
9	LRGH	Empirical	28	0	± 0.029
10	Yun-San	Empirical	29	0	± 0.032
11	S-	Mechanistic	9, 11, 12	0	± 0.034
12	Chen	Semi-empirical	22	0	± 0.069
13	Cubic Cell	Mechanistic	13	0	± 0.102

Table 4 22 Dry Canadian soils (fine)

#	Model name	Model type	Equations	M	SD ($Wm^{-1} \cdot K^{-1}$)
1	GSC	Empirical	25	0	± 0.016
2	MaxRTCM	Mechanistic	38–40	1	± 0.018
3	CDry-40	Empirical	30	2	± 0.018
4	C–B ($u = 0.445$)	Semi-empirical	20	1	± 0.021
5	Yun-San	Empirical	29	0	± 0.025
6	LRGH	Empirical	28	0	± 0.026
7	C–K	Empirical	27	0	± 0.026
8	A-GMM	Semi-empirical	17	1	± 0.028
9	S-	Mechanistic	9, 11, 12	0	± 0.042
10	deVries Model	Mechanistic	3 and 4	1	± 0.044
11	deVries-ave	Semi-empirical	35	1	± 0.055
12	Chen	Semi-empirical	22	0	± 0.080
13	Cubic Cell	Mechanistic	13	0	± 0.087

6.1.1 Model Assessment

Overall, the closest λ_{dry} predictions to experimental data were made by MaxRTCM (Eqs. 38–40). The MaxRTCM average prediction error, $|\lambda_{dry-cal} - \lambda_{dry-exp}| / \lambda_{dry-ave}$, for the 18 coarse soils, with respect to their average $\lambda_{dry-exp}$ value of $0.247 Wm^{-1} \cdot K^{-1}$, was about 5.3%, while, for the 22 fine soils, with respect to their average $\lambda_{dry-exp}$ value of $0.199 Wm^{-1} \cdot K^{-1}$, was about 6.3%. For coarse soils, the largest over-prediction of 14% was noted for ON-05 soil and the worst

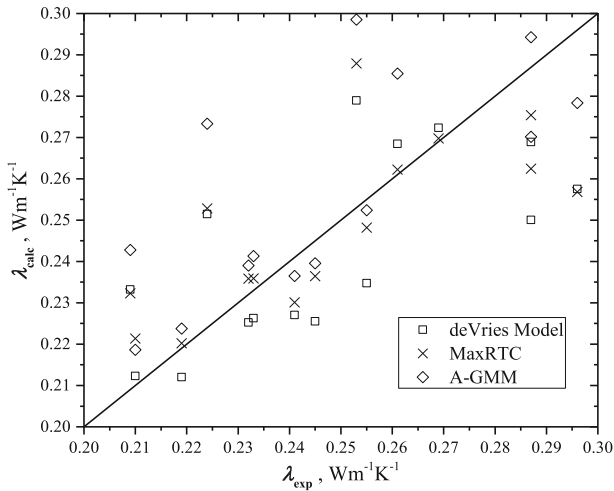


Fig. 4 18 Canadian coarse dry soils: $\lambda_{\text{dry-cal}}$ versus λ_{exp}

under-prediction of 16% was noted for PE-03 soil. For fine soils, the largest over-prediction was noted for NB-04 soil (18.7%) and the worst under-prediction was for ON-01 soil at 28.3%. For all 40 Canadian soils, the overall *SD* for MaxRTCM was $\pm 0.018 \text{ Wm}^{-1} \cdot \text{K}^{-1}$ which is equivalent to about 8.2% error in λ_{dry} predictions with respect to the average value of $\lambda_{\text{dry-exp}}$ ($0.220 \text{ Wm}^{-1} \cdot \text{K}^{-1}$). The obtained results closely followed experimental data and indicated a positive influence of the correlated $f_{\text{sc-cor}}$ on the model performance, when applied to dry soils.

When the deVries Model (Eqs. 3 and 4) is applied separately to coarse and fine soils, it produces an *SD* of $\pm 0.022 \text{ Wm}^{-1} \cdot \text{K}^{-1}$ and $\pm 0.044 \text{ Wm}^{-1} \cdot \text{K}^{-1}$ for coarse and fine soils, respectively.

Hence, λ_{dry} estimates for fine soils by the deVries Model do not follow experimental data well (Figs. 4 and 5).

The S-|| model (Eq. 9) delivers λ_{dry} estimates at $\pm 0.034 \text{ Wm}^{-1} \cdot \text{K}^{-1}$ and $\pm 0.042 \text{ Wm}^{-1} \cdot \text{K}^{-1}$ for coarse and fine soils, respectively. The Cubic Cell model (Eq. 13) under estimates λ_{dry} data for coarse and fine soils ($-0.102 \text{ Wm}^{-1} \cdot \text{K}^{-1}$ and $-0.087 \text{ Wm}^{-1} \cdot \text{K}^{-1}$, respectively).

Among four semi-empirical (deVries-ave, C-B, A-GMM and Chen) and five empirical equations (GSC, C-K, LRGH, Yun, and CDry-40), the best estimates were obtained by CDry-40, i.e., Eq. 30 ($\pm 0.021 \text{ Wm}^{-1} \cdot \text{K}^{-1}$ and $\pm 0.018 \text{ Wm}^{-1} \cdot \text{K}^{-1}$ for coarse and fine soils, respectively), closely followed by C-B and GSC, and A-GMM estimates. In turn, deVries-ave (Eqs. 34 and 35) gives $\pm 0.023 \text{ Wm}^{-1} \cdot \text{K}^{-1}$ and $\pm 0.055 \text{ Wm}^{-1} \cdot \text{K}^{-1}$ for coarse and fine soils, respectively; therefore, there is no significant difference in using the full deVries Model or its simplified version, deVries-ave.

With respect to CDry-40 (Eq. 30), its predictive performance (Eq. 41) is degraded due to a higher number of fitted coefficients ($M = 2$), while MaxRTCM and A-GMM require just one fitting coefficient ($M = 1$). In addition, a brief review of Tables 3 and 4

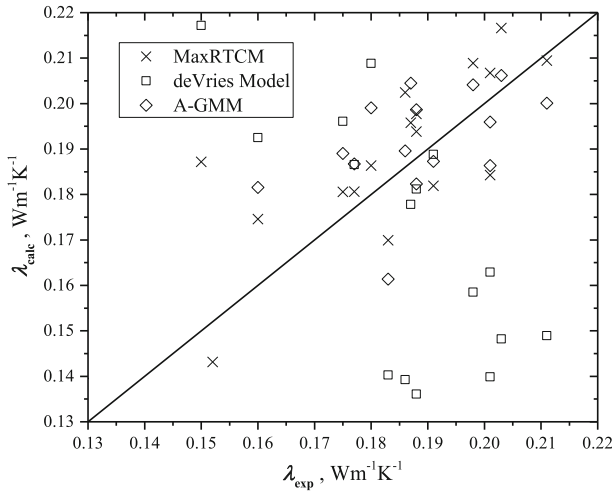


Fig. 5 22 Canadian fine dry soils: $\lambda_{\text{dry-cal}}$ versus λ_{exp}

Table 5 Saturated 18 Canadian soils (coarse)

#	Model name	Model type	Equations	<i>M</i>	<i>SD</i> ($\text{Wm}^{-1} \cdot \text{K}^{-1}$)
1	A-GMM	Semi-empirical	18	0	± 0.085
2	S-	Mechanistic	10, 11, 12	0	± 0.107
3	C-B	Semi-empirical	20	1	± 0.111
4	deVries Model	Mechanistic	5, 6	1	± 0.115
5	Cubic Cell	Mechanistic	13	0	± 0.154
6	GSC	Empirical	26	0	± 0.261
7	CSat-18	Empirical	31	3	± 0.315
8	deVries-ave	Semi-empirical	36	1	± 0.331

revealed that the *SD* of the top 10 λ_{dry} models varied in a narrow range (from ± 0.014 to $\pm 0.028 \text{ Wm}^{-1} \cdot \text{K}^{-1}$). This suggests that simplicity could be a dominating factor when choosing a model. In reality, the requirement of simplicity is not met by the MaxRTCM and deVries models, but it is met by CDry-40 (Eq. 30).

6.2 Saturated Soils

Tables 5 and 6 summarize the predictive performances of eight λ_{sat} models, for 18 coarse and 22 fine soils, respectively.

With respect to CSat-18 and CSat-22 (Eqs. 31 and 32), it is worth to mention that their predictive performance (Eq. 41) is lowered due to the use of a high number of fitted coefficients ($M = 3$), while the two best models, A-GMM and S-||, do not require any fitting coefficients ($M = 0$) to the 40-Canadian soil data.

Table 6 Saturated 22 Canadian soils (fine)

#	Model name	Model type	Equations	<i>M</i>	<i>SD</i> ($\text{Wm}^{-1} \cdot \text{K}^{-1}$)
1	A-GMM	Semi-empirical	18	0	± 0.113
2	S-	Mechanistic	10–12	0	± 0.128
3	CSat-22	Empirical	32	3	± 0.135
4	Cubic Cell	Mechanistic	13	0	± 0.138
5	C–B	Semi-empirical	20	1	± 0.179
6	deVries Model	Mechanistic	5, 6	1	± 0.229
7	deVries-ave	Semi-empirical	37	1	± 0.251
8	GSC	Empirical	26	0	± 0.263

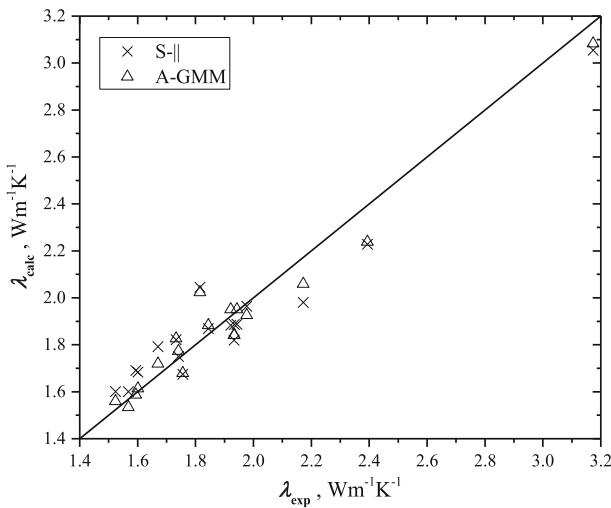


Fig. 6 18 Canadian saturated coarse soils: $\lambda_{\text{sat-calc}}$ versus λ_{exp}

Figures 6 and 7 display the λ_{sat} estimates of the two best models versus experimental data. It appears that the models estimate experimental λ_{sat} quite well. In reality, their *SD* values are bigger than those for λ_{dry} (Tables 5 and 6 vs. 3 and 4). However, due to much larger λ_{sat} values with respect to λ_{dry} , the relative errors of λ_{sat} estimates are relatively small. For example, for coarse soils, the largest over-prediction by A-GMM of 6.4 % was noted for SK-04 soil and the worst under-prediction of 11.4 % was noted for NS-05 soil. For fine soils, the largest over-prediction by A-GMM was noted for NB-04 soil (14.8 %) and the worst under-prediction was for MN-02 soil at 15.6 %.

7 Model Verification Versus Other Soils

The extension of each model under scrutiny to other soils was evaluated by comparison of their estimates against λ data of 21 other soils, listed in Table 4. Among them, coarse

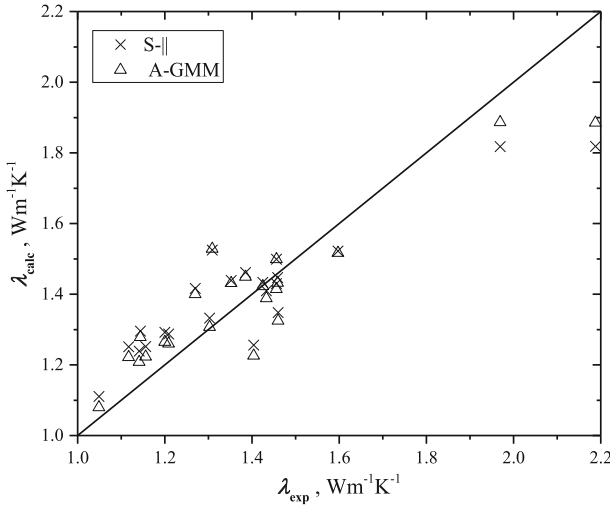


Fig. 7 22 Canadian saturated fine soils: $\lambda_{\text{sat-calc}}$ versus λ_{exp}

soils were represented by Ottawa sands (C109 and C190), Toyoura sand, Pozzolana soil, five Chinese soils and Tottori sand, while fine soils were represented by five Chinese and two Japanese soils. The physical characteristics of these soils are displayed in Table 7.

The *SD* of the best six models of λ_{dry} are displayed in Table 8 (coarse soils) and Table 9 (fine soils), while the same for λ_{sat} is displayed in Table 10 (coarse soils) and Table 11 (fine soils). None of the models were fitted to λ data of these 21 soils; consequently, $M = 0$.

For dry coarse soils, the best λ_{dry} estimates are given by mechanistic models (MaxRTCM and deVries Model).

For fine soils, the top ranking models were LRGH (fitted to λ_{dry} data of 10 Chinese soils) and A-GMM. Tables 8 and 9 show a narrow range of *SD* which suggests that there is no significant advantage among any of the listed models for both coarse and fine soils tested. However, from Tables 8 and 9 in conjunction with Tables 3 and 4, it can be seen in MaxRTCM model consistently appears on or near the top in the ranking lists as the best model for estimating λ_{dry} of soils.

From Table 10 (saturated coarse other soils) and Table 11 (saturated fine other soils), the best λ_{sat} estimates were given by S-|| or A-GMM models for both coarse and fine soils. However, unlike λ_{dry} , Tables 10 and 11 in conjunction with Tables 5 and 6 show a wide range of *SD* which suggests that S-|| and A-GMM models are in general the best models for estimating λ_{sat} of soils.

8 Summary of Model Performance

The thermal conductivity data of 40 Canadian soils at dryness and full saturation were used to verify commonly applied λ_{dry} and λ_{sat} models of mechanistic,

Table 7 Physical characteristics of 21 other soils

Soil code	Refs.	m_{sa}	m_{si}	m_{cl}	θ_{qtz}	ρ_b (kg · m ⁻³)	n	λ_s (Wm ⁻¹ · K ⁻¹)	$\lambda_{dry-exp}$ (Wm ⁻¹ · K ⁻¹)	$\lambda_{sat-exp}$ (Wm ⁻¹ · K ⁻¹)
C-109	[5]	1.00	0.00	0.00	1.00	1802	0.32	7.70	0.33	3.37
C-109	[5]	1.00	0.00	0.00	1.00	1590	0.40	7.70	0.25	2.93
C-190	[5]	1.00	0.00	0.00	1.00	1802	0.32	7.70	0.33	3.42
C-190	[5]	1.00	0.00	0.00	1.00	1590	0.40	7.70	0.25	2.88
Toyoura Sand	[15]	1.00	0.00	0.00	0.87	1643	0.38	6.48	0.27	2.69
Toyoura Sand	[15]	1.00	0.00	0.00	0.87	1590	0.40	6.48	0.25	2.63
Pozzolana	[28]	0.55	0.45	0.00	0.00	1549	0.44	2.16	0.23	1.20
Pozzolana	[28]	0.55	0.45	0.00	0.00	1383	0.50	2.16	0.19	1.14
S-Ren-001	[12]	0.94	0.01	0.05	0.74	1598	0.41	5.44	0.25	2.20
S-Ren-002	[12]	0.93	0.01	0.06	0.51	1600	0.41	3.99	0.27	1.88
S-Ren-003	[12]	0.67	0.21	0.12	0.64	1390	0.49	4.73	0.23	1.73
S-Ren-004	[12]	0.40	0.49	0.11	0.55	1301	0.52	4.21	0.18	1.53
S-Ren-011	[12]	0.50	0.41	0.09	0.57	1381	0.49	4.28	0.22	1.48
Tottori sand	[25]	0.92	0.05	0.03	0.52	1550	0.42	2.50	0.15	1.40
Silt loam-5	[12]	0.27	0.51	0.22	0.47	1332	0.51	3.77	0.20	1.60
Silt loam-6	[12]	0.11	0.70	0.19	0.62	1304	0.52	4.60	0.22	1.33
Silty clay loam-7	[12]	0.19	0.54	0.27	0.34	1300	0.52	3.18	0.24	1.35
Silty clay loam-8	[12]	0.08	0.60	0.32	0.36	1299	0.52	3.27	0.20	1.38
Clay loam-9	[12]	0.32	0.38	0.30	0.41	1293	0.52	3.45	0.24	1.63
Red-Yellow	[15]	0.34	0.23	0.43	0.58	1080	0.60	4.43	0.16	1.30

Table 8 Ranking of λ_{dry} models (14 coarse other soils)

#	Model name	Model type	Equations	M	SD ($\text{Wm}^{-1} \cdot \text{K}^{-1}$)
1	MaxRTCM	Mechanistic	38, 39, 40	0	± 0.027
2	deVries Model	Mechanistic	3, 4	0	± 0.028
3	C–K	Empirical	27	0	± 0.028
4	S-	Mechanistic	9	0	± 0.029
5	deVries-ave	Semi-empirical	34	0	± 0.029
6	CDry-40	Empirical	30	0	± 0.032

Table 9 Ranking of λ_{dry} models (7 fine other soils)

#	Model name	Model type	Equations	M	SD ($\text{Wm}^{-1} \cdot \text{K}^{-1}$)
1	LRGH	Empirical	28	0	± 0.022
2	A-GMM	Semi-empirical	17	0	± 0.024
3	Yun-San	Empirical	29	0	± 0.024
4	MaxRTCM	Mechanistic	38, 39, 40	0	± 0.028
5	CDry-40	Empirical	30	0	± 0.028
6	GSC	Empirical	25	0	± 0.032

Table 10 Ranking of λ_{sat} models (14 coarse soils)

#	Model name	Model type	Equations	M	SD ($\text{Wm}^{-1} \cdot \text{K}^{-1}$)
1	A-GMM	Semi-empirical	18	0	± 0.075
2	S-	Mechanistic	10	0	± 0.079
3	deVries Model	Mechanistic	5, 6	0	± 0.097
4	C–B	Semi-empirical	20	0	± 0.165
5	Cubic Cell	Mechanistic	13	0	± 0.280
6	GSC	Empirical	26	0	± 0.281

Table 11 Ranking of λ_{sat} models (7 fine soils)

#	Model name	Model type	Equations	M	SD ($\text{Wm}^{-1} \cdot \text{K}^{-1}$)
1	S-	Mechanistic	10	0	± 0.135
2	A-GMM	Semi-empirical	18	0	± 0.145
3	Cubic Cell	Mechanistic	13	0	± 0.145
4	deVries-ave	Semi-empirical	37	0	± 0.189
5	CSat-22	Empirical	32	0	± 0.240
6	C–B	Semi-empirical	20	0	± 0.251

semi-empirical and empirical types. For mechanistic models, applied to dry soils, the closest λ_{dry} estimates were given by MaxRTCM ($SD = 0.018 \text{ Wm}^{-1} \cdot \text{K}^{-1}$ for the 40 Canadian soils). The deVries Model also provided good estimates ($\pm 0.022 \text{ Wm}^{-1} \cdot \text{K}^{-1}$), but only for 18 coarse Canadian soils. The S-|| model gave satisfactory estimates ($\pm 0.034 \text{ Wm}^{-1} \cdot \text{K}^{-1}$ and $\pm 0.042 \text{ Wm}^{-1} \cdot \text{K}^{-1}$, for coarse and fine soils, respectively). The Cubic Cell Model largely underestimated experimental λ (i.e., $-0.102 \text{ Wm}^{-1} \cdot \text{K}^{-1}$ and $-0.087 \text{ Wm}^{-1} \cdot \text{K}^{-1}$, for coarse and fine soils, respectively). From four semi-empirical equations: deVries-ave, A-GMM, C-B and Chen's equation, the best λ_{dry} estimates were given by C-B model ($\pm 0.021 \text{ Wm}^{-1} \cdot \text{K}^{-1}$ and $\pm 0.021 \text{ Wm}^{-1} \cdot \text{K}^{-1}$, for coarse and fine soils, respectively). The A-GMM model also produced acceptable predictions ($\pm 0.029 \text{ Wm}^{-1} \cdot \text{K}^{-1}$ and $\pm 0.028 \text{ Wm}^{-1} \cdot \text{K}^{-1}$, for coarse and fine soils, respectively). Finally, deVries-ave produced good estimates for coarse soils ($\pm 0.023 \text{ Wm}^{-1} \cdot \text{K}^{-1}$). Among five empirical equations, the best estimates were given by CDry-40 ($\pm 0.021 \text{ Wm}^{-1} \cdot \text{K}^{-1}$ and $\pm 0.018 \text{ Wm}^{-1} \cdot \text{K}^{-1}$, for coarse and fine soils, respectively) and GSC ($\pm 0.023 \text{ Wm}^{-1} \cdot \text{K}^{-1}$ and $\pm 0.016 \text{ Wm}^{-1} \cdot \text{K}^{-1}$, for coarse and fine soils, respectively). For 18 coarse Canadian soils at saturation, the best λ_{sat} estimates were given by A-GMM ($\pm 0.085 \text{ Wm}^{-1} \cdot \text{K}^{-1}$) and S-|| model ($\pm 0.107 \text{ Wm}^{-1} \cdot \text{K}^{-1}$), while, for 22 fine Canadian soils at saturation, the best λ_{sat} data were also produced by A-GMM ($\pm 0.113 \text{ Wm}^{-1} \cdot \text{K}^{-1}$) and S-|| model ($\pm 0.128 \text{ Wm}^{-1} \cdot \text{K}^{-1}$).

In addition, λ_{sat} and λ_{dry} models, without fitting parameters ($M = 0$), were applied to λ data of 21 other soils. Testing results for λ_{dry} models revealed a good performance for MaxRTCM ($\pm 0.025 \text{ Wm}^{-1} \cdot \text{K}^{-1}$ for 14 coarse soils and $\pm 0.027 \text{ Wm}^{-1} \cdot \text{K}^{-1}$ for 7 fine soils). The MaxRTCM model performance was followed by CDry-40 ($\pm 0.033 \text{ Wm}^{-1} \cdot \text{K}^{-1}$ and $\pm 0.029 \text{ Wm}^{-1} \cdot \text{K}^{-1}$, respectively), LRGH ($\pm 0.043 \text{ Wm}^{-1} \cdot \text{K}^{-1}$ and $\pm 0.022 \text{ Wm} \cdot \text{K}^{-1}$, respectively), GSC ($\pm 0.038 \text{ Wm}^{-1} \cdot \text{K}^{-1}$ and $\pm 0.032 \text{ Wm}^{-1} \cdot \text{K}^{-1}$, respectively), S-|| ($\pm 0.029 \text{ Wm}^{-1} \cdot \text{K}^{-1}$ and $\pm 0.041 \text{ Wm}^{-1} \cdot \text{K}^{-1}$, respectively), and deVries ($\pm 0.028 \text{ Wm}^{-1} \cdot \text{K}^{-1}$ and $\pm 0.044 \text{ Wm}^{-1} \cdot \text{K}^{-1}$, respectively). The closest estimation of λ_{sat} for 14 coarse soils was given by A-GMM and S-|| model ($\pm 0.0747 \text{ Wm}^{-1} \cdot \text{K}^{-1}$ and $\pm 0.0795 \text{ Wm}^{-1} \cdot \text{K}^{-1}$, respectively), while the closest estimation for 7 fine soils was given by S-|| model and A-GMM ($\pm 0.1354 \text{ Wm}^{-1} \cdot \text{K}^{-1}$ and $\pm 0.1451 \text{ Wm}^{-1} \cdot \text{K}^{-1}$, respectively).

9 Conclusions

Among the mechanistic λ_{dry} models discussed, only MaxRTCM provided acceptable estimates for 40 Canadian soils as well as the 21 other soils. It appears that the use of $f_{\text{sc-cor}}$ benefitted the model performance, when applied to dry soils. However, the complex structure of this model is a discouraging factor.

Also, there was no SD difference between the full model by de Vries and its simplified version (deVries-ave) when applied to 18 Canadian coarse soils.

A brief review of the ranking tables for dry soils revealed that for the majority of models, SD varied over a narrow range, whereas, for saturated soils, SD varied over a much wider range. This suggests that in real dry soil applications, simple models can be a preferable choice, rather than MaxRTCM. For example, CDry-40 offers close predictions against λ_{dry} data of the 40 Canadian soils and the 21 other soils. As far as λ_{sat} models are concerned, only A-GMM and S-|| models provide good estimates when applied to 40 Canadian soils as well as the 21 other soils. There are also slight differences in the model ranking obtained for 40 Canadian versus 21 other soils. These small irregularities are probably due to missing mineral composition data for Chinese and some Japanese soils; consequently, rough λ_s estimates were used. In addition, for 21 other soils, often rough m_{sa} estimates were used to assess parameters such as the quartz content.

With respect to mechanistic (physics based) models, their advantage is in their hypothetical flexibility of application to any soil data. However, they are based on very simplified assumptions regarding soil structure and heat and mass transfer phenomena involved. They are complex in form and often are packed with coefficients that are hard to determine; consequently, they are fitted to soil experimental data. In conclusion, when applied to soils with incomplete characteristics (e.g., grain size distribution, n and mineral data), these models are likely prone to be bias. Therefore, there is a need for new models and more reliable experimental data of soils. Subsequently, more study is needed on soil systems made of solid minerals and air/water, with an inclusion of inter-particle thermal contact resistance.

Appendix

See Table 12.

Table 12 Selected soil minerals and their approximate λ_{min} values

Mineral	λ_{min} [29] ($Wm^{-1} \cdot K^{-1}$)	Mineral	λ_{min} [30] ($Wm^{-1} \cdot K^{-1}$)
Quartz (qtz)	7.7 ± 0.88	K-feldspar (Kfs)	2.3 ± 0.21
Chlorite (chl)	3.26 ± 0.25	Amphibole (am)	2.81 ± 0.27
Kaolinite (kln)	2.64 ± 0.20	Albite (ab)	2.14 ± 0.19
Calcite (cal)	3.26 ± 0.23	Goethite (gt)	2.91
Dolomite (dol)	5.33 ± 0.26	Haematite (hem)	12.42 ± 1.74
Illite (ill)	1.85 ± 0.23		
Smectite (sme)	1.88 ± 0.15		

References

1. O.T. Farouki, *Thermal Properties of Soils* (Trans Tech Publications, Clausthal-Zellerfeld, 1986)
2. O. Johansen, *Thermal Conductivity of Soils, Corps of Engineers* (U.S. Army, Cold Regions Research and Engineering Laboratory, Hanover, 1977)
3. G. Bovesecchi, P. Coppa, Basic problems in thermal-conductivity measurements of soils. *Int. J. Thermophys.* **34**, 1962–1974 (2013). <https://doi.org/10.1007/s10765-013-1503-2>
4. G. Bovesecchi, P. Coppa, M. Potenza, A numerical model to explain experimental results of effective thermal conductivity measurements on unsaturated soils. *Int. J. Thermophys.* **38**, 68 (2017). <https://doi.org/10.1007/s10765-017-2202-1>
5. T.S. Yun, J.C. Santamarina, Fundamental study of thermal conduction in dry soils. *Granular Matter* **10**, 197–207 (2008). <https://doi.org/10.1007/s10035-007-0051-5>
6. W.L. Vargas, J.J. McCarthy, Heat conduction in granular materials. *AIChE J.* **47**, 1052–1059 (2001). <https://doi.org/10.1002/aic.690470511>
7. V.R. Tarnawski, T. Momose, W.H. Leong, G. Bovesecchi, P. Coppa, Thermal conductivity of standard sands. Part I. Dry-state conditions. *Int. J. Thermophys.* **30**, 949–968 (2009). <https://doi.org/10.1007/s10765-009-0596-0>
8. D.R. Chaudhary, R.C. Bhandari, Heat transfer through a three-phase porous medium. *J. Phys. D Appl. Phys.* **1**, 815–817 (1968). <https://doi.org/10.1088/0022-3727/1/6/418>
9. G.S. Campbell, *Soil Physics with BASIC: Transport Models for Soil-Plant Systems* (Elsevier, New York, 1985). ISBN 9780080869827
10. S.X. Chen, Thermal conductivity of sands. *J. Heat Mass Transf.* **44**, 1241–1246 (2008). <https://doi.org/10.1007/s00231-007-0357-1>
11. J. Côté, J.M. Konrad, A generalized thermal conductivity model for soils and construction materials. *Can. Geotech. J.* **42**, 443–458 (2005). <https://doi.org/10.1139/t04-106>
12. S. Lu, T. Ren, Y. Gong, R. Horton, An improved model for predicting soil thermal conductivity from water content at room temperature. *Soil Sci. Soc. Am. J.* **71**, 8–14 (2007). <https://doi.org/10.2136/sssaj2006.0041>
13. D.A. De Vries, Thermal properties of soils, in *Physics of Plant Environment*, ed. by W.R. van Wijk (North-Holland, Amsterdam, 1963), pp. 210–235
14. W. Woodside, J.H. Messmer, Thermal conductivity of porous media. I. Unconsolidated sands. *J. Appl. Phys.* **32**, 1688–1699 (1961). <https://doi.org/10.1063/1.1728419>
15. T. Kasubuchi, T. Momose, F. Tsuchiya, V.R. Tarnawski, Normalized thermal conductivity model for three Japanese soils. *Trans. Jpn. Soc. Irrig. Drain. Reclam. Eng.* **251**, 53–57 (2007). ISSN: 18822789
16. V.R. Tarnawski, W.H. Leong, A series-parallel model for estimating the thermal conductivity of unsaturated soils. *Int. J. Thermophys.* **33**, 1191–1218 (2012). <https://doi.org/10.1007/s10765-012-1282-1>
17. F. Gori, S. Corasaniti, Theoretical prediction of the thermal conductivity and temperature variation inside mars soil analogues. *Planet. Space Sci.* **52**, 91–99 (2004). <https://doi.org/10.1016/j.pss.2003.08.009>
18. F. Gori, S. Corasaniti, New model to evaluate the effective thermal conductivity of three-phase soils. *Int. Commun. Heat Mass* **47**, 1–6 (2013). <https://doi.org/10.1016/j.icheatmasstransfer.2013.07.004>
19. S.E. Wood, Analytical model for thermal conductivity (kth) of planetary regolith: uncemented, cohesive or compressed, non-spherical particles, in *Proceedings of 44th Lunar and Planetary Science Conference: The Woodlands*, Texas, March 18–22 (2013)
20. V.R. Tarnawski, W.H. Leong, Advanced geometric mean model for predicting thermal conductivity of unsaturated soils. *Int. J. Thermophys.* **37**, 18 (2016). <https://doi.org/10.1007/s10765-015-2024-y>
21. J. Sundberg, Thermal properties of soils and rocks. *Geologiska Institutionen A57*, 1–310 (1988). ISSN: 0348-2367
22. L.S. Fletcher, Recent developments in contact conductance heat transfer. *J. Heat Transf.* **110**, 1059–1070 (1988). <https://doi.org/10.1115/1.3250610>
23. V.R. Tarnawski, T. Momose, M.L. McCombie, W.H. Leong, Canadian field soils III. Thermal-conductivity data and modeling. *Int. J. Thermophys.* **36**, 119–156 (2015). <https://doi.org/10.1016/j.ijheatmasstransfer.2008.07.037>
24. J. Côté, J.M. Konrad, Assessment of structure effects on the thermal conductivity of two-phase porous geomaterials. *Int. J. Heat Mass Transf.* **52**, 796–804 (2009). <https://doi.org/10.1016/j.ijheatmasstransfer.2008.07.037>

25. V.R. Tarnawski, T. Momose, W.H. Leong, B. Wagner, Performance evaluation of soil thermal conductivity models, in *Proceedings of the ASME-ATI-UIT 2010 Conference Thermal and Environmental Issues in Energy Systems*, Sorrento, Italy, June 21–23 (2010)
26. M.S. Kersten, Thermal Properties of Soils. Bulletin 28. University of Minnesota (1949). <http://hdl.handle.net/11299/124271>
27. W.C. Krumbein, L.L. Sloss, *Stratigraphy and Sedimentation* (Freeman and Co., San Francisco, 1956)
28. M.L. McCombie, V.R. Tarnawski, G. Bovesecchi, P. Coppa, W.H. Leong, Thermal conductivity of pyroclastic soil (Pozzolana) from the environs of Rome. *Int. J. Thermophys.* **38**, 21 (2017). <https://doi.org/10.1007/s10765-016-2161-y>
29. F. Brigaud, G. Vasseur, Mineralogy, porosity and fluid control on thermal conductivity of sedimentary rocks. *Geophys. J. Int.* **98**, 525–542 (1989). <https://doi.org/10.1111/j.1365-246X.1989.tb02287.x>
30. Ch. Clauser, E. Huenges, Thermal conductivity of rocks and minerals, in *Rock Physics & Phase Relations: A Handbook of Physical Constants*. American Geophysical Union, 105–126 (1995). <https://doi.org/10.1029/RF003p0105>